Atmos. Chem. Phys. Discuss., doi:10.5194/acp-2015-913, 2016
Manuscript under review for journal Atmos. Chem. Phys.
Published: 22 January 2016

Atmospheric Chemistry and Physics Discussions

A DNS study of aerosol and small-scale cloud turbulence interaction

N. Babkovskaia[1], U. Rannik[1], V. Phillips[2], H. Siebert[3], B. Wehner[3], and M. Boy[1]

[1]University of Helsinki, Department of Physics, Helsinki, Finland
[2]Lund University, Department of Physical Geography and Ecosystems Science, Sweden
[3]Leibniz Institute for Tropospheric Research, Leipzig, Germany

Correspondence to: N. Babkovskaia
(NBabkovskaia@gmail.com)

Abstract. The purpose of this study is to investigate the effect of aerosol dynamics (evaporation/condensation) on atmospheric small-scale turbulence (and vice versa) using direct numerical simulations (DNS). We consider the domain located on the height of about 2000 m from the sea level, experiencing transient high supersaturation due to atmospheric fluctuations of temperature and humidity. To study the effect of aerosol dynamics on the turbulence we vary the total number of particles (N_{tot}). In turn, to investigate the effect of small-scale turbulence on evolution of aerosol particles we vary the intensity of turbulent fluctuations and the buoyant force. We find that even small amount of aerosol particles (55.5 cm^{-3}) increases the air temperature by 1 K under supersaturated conditions due to release of latent heat. The system comes to an equilibrium faster and the relative number of activated particles appears to be smaller for larger N_{tot} . We conclude that the presence of aerosol particles results in deceleration of air motion in vertical direction and damping of turbulent fluctuations.

1 Introduction

Interaction of atmospheric turbulence with aerosol and cloud formation processes has been studied extensively. Due to non-linearity of particle formation and other aerosol dynamical processes, the fluctuations of temperature and relative humidity can have strong effect on aerosol formation. Large scale fluctuations of atmospheric properties, which occur for example in the atmospheric boundary layer, can be the drivers for initiation of particle formation (Easter et al., 1994). Mixing of air with different properties, including temperature and relative humidity, have been shown to enhance atmospheric nucleation significantly (Nilsson and Kulmala, 1998). More specifically, the atmospheric waves can increase the nucleation rate several orders of magnitude and affect also the size spectum of the particles (Nilsson et al., 2000). Also the activation of atmospheric particles in cloud areas is affected by the fluctuation of supersaturation, where some droplets were shown to grow also in undersaturated conditions due to fluctuations and the bi-modal particle size distribution could be observed after initially unimodal particle population experienced fluctuating supersaturation (Kulmala et al., 1997).

In-cloud turbulence has been shown to intensify cloud-microphysical processes determining cloud properties (Benmoshe and Khain, 2014). Similarly, aerosol loadings also influence the numbers and sizes of cloud-particles, thereby influencing precipitation of formation, cloud extent and hence the climate (Forster, 2007). Both turbulence and aerosol particles can influence the chemical reactions in the atmosphere providing surfaces for aqueous phase chemistry and promoting uptake of gaseous species. This can have repercussions for chemical reactions in the air. Yet both environmental factors, namely aerosol composition and turbulence, have been usually considered as separate influences.

The large-scale atmospheric turbulence is well known to affect aerosol processes significantly. In turn, aerosol properties may influence the buoyancy and turbulence. A motivation for a potential aerosol-turbulence interaction is that the most advanced cloud-microphysical models can now resolve the cloud edges where mixing occurs and where spatial gradients are great in turbulence and concentrations of hydrometeors, including aerosols. Consequently, by including a more complete set of such interactions in the models, a better simulation of aerosols, turbulence and microphysics may be possible.

The main goal of this direct numerical simulation (DNS) study is to investigate interaction between small-scale turbulence and aerosol and cloud microphysical properties.

Atmos. Chem. Phys. Discuss., doi:10.5194/acp-2015-913, 2016
Manuscript under review for journal Atmos. Chem. Phys.
Published: 22 January 2016

Atmospheric Chemistry and Physics Discussions

case 1	$N_{tot} = 55.5$ cm^{-3}
case 2	$N_{tot} = 555$ cm^{-3}
case 3	$N_{tot} = 5550$ cm^{-3}
case 4	no particles

Table 1. The following cases are considered in this study.

	equilibrium	*unequilibrium*
low intensive turbulence	$T_0 = 285.4$ K $f_0 = 10$	$T_0 = 293$ K $f_0 = 10$
high intensive turbulence	$T_0 = 285.4$ K $f_0 = 100$	$T_0 = 293$ K $f_0 = 100$

Table 2. The summary of key parameters for studying the effect of aerosol on turbulence. All four sets of parameters are used to compare cases *1* and *4* (see Table 1).

The choosen DNS domain is realistic for a small volume at cloud edge where turbulent mixing is a dominat feature (Katzwinkel et al., 2014) and can create fluctuations in temperature as well as humidity. Such conditions however appear transient because presence of atmospheric aerosols leads to depletion of supersaturation via condensation and droplet activation.

We use the high order public domain finite difference PENCIL Code for compressible hydrodynamic flows. The code is highly modular and comes with a large selection of physics modules. It is widely documented in the literature (Dobler et al., 2006; Pencil Code, 2001, and references therein). The chemistry module is responsible for the detailed description of the necessary quantities in a case of complicated chemical composition, such as diffusion coefficients, thermal conductivity, reaction rates etc. (Babkovskaia et al., 2011). The detailed description of aerosol module is in Babkovskaia et al. (2015). The paper is constructed as follows. Section 2 is devoted to the description of the model. Results are presented in Section 3. Section 4 is the summary.

2 Description of the model

Aerosol

As a starting point for our simulations we consider values typical for observations made in trade wind cumuli. During the CARRIBA project (Siebert et al. 2013, hereafter called SI13) total aerosol number concentrations in the marine sub-cloud layer up to a few 100 cm^{-3} have been observed (Fig 6f in SI13). Although it was argued that the highest values are due to local biomass burning we consider a concentration of 550 cm^{-3} as typical and 55 and 5550 cm^{-3} as two extreme values for sensitivity test. The initial normalized aerosol number size distribution as shown as a dotted line in Fig. 3 in our manuscript compares well with the shape of the observed distribution shown as red line in Fig. 8 of SI13.

We assume a soluble aerosol (NaCl) which will dilute inside droplet. We take 50 size bins logarithmically distributed in the range [10 nm, 1000 μm]. As an initial distribution of particles we take the observational data at the sea level and assume that it is the same everywhere in the domain (see the distribution in Fig. 3). To analyse the effect of total number of aerosol particles, N_{tot}, on the structure and properties of turbulent motion we consider the following cases: $N_{tot} = 55.5$ cm^{-3} (*case 1*), $N_{tot} = 555$ cm^{-3} (observed data, *case 2*), $N_{tot} = 5550$ cm^{-3} (*case 3*), and no particles (*case 4*), see Table 1.

Air composition

We assume the following air composition O_2 + H_2O + N_2, where nitrogen mass fraction is taken to be $Y_{N_2} = 70\%$. The observations provide us the absolute humidity to set the initial value for mass fraction of water vapour, Y_{H_2O}. Oxygen mass fraction is recalculated from the normalization conditions, i.e. $Y_{O_2} + Y_{H_2O} + Y_{N_2} = 1$, where Y_{O_2} is oxygen mass fraction.

Initial conditions

Based on data of CARRIBA observations typical for the upper parts of clouds / cloud edges in a height of 2000 m, we set the initial conditions for air temperature ($T_0 = 285.4$ K) and water vapour mixing ratio ($q_0 = 0.0124$). The small vertical gradients of temperature ($\Delta T = 0.001$ K) and water content ($\Delta q = 4 \times 10^{-5}$) are also based on the CARRIBA measurements.

Direct observations of supersaturation fluctuations are not possible so far and one has to rely on estimates based on measurements of air temperature and water vapor mixing ratio. The measured temperature and absolute humidity led us to a range of supersaturation (S) from 10.17 % to 10.54 %. Such values of S are extremely high in a case of an adiabatic lifting of a cloudy air parcel. The "quasi-steady state" supersaturation depends mainly on vertical updraft velocity and appears to be on the order of a few tenths of percent for vertical updrafts of about 1 m s^{-1}. However, it is well known that atmospheric clouds are mainly non-adiabatic due to turbulent mixing, and a few percent supersaturation are realistic for higher updraft velocities (e.g., Korolev and Mazin, 2003). This is particular true at cloud edges where entrainment of unsaturated air into the cloud results in strong mixing and fluctuations of the water vapor and temperature field. It strongly depends on the correlation between these two thermodynamic fields whether strong fluctuations can result in high fluctuations of supersaturation or not. Until now we are not aware of any observations of this correlation in clouds. Based on theoretical arguments and observations in the convective boundary layer below clouds Kulmala et al. (1997)

Atmos. Chem. Phys. Discuss., doi:10.5194/acp-2015-913, 2016
Manuscript under review for journal Atmos. Chem. Phys.
Published: 22 January 2016

Atmospheric Chemistry and Physics Discussions

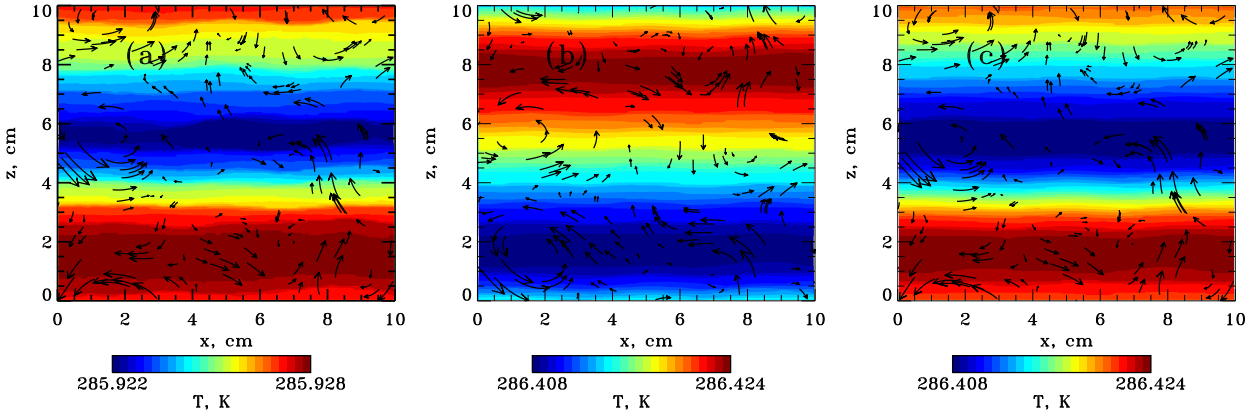

Fig. 1. Temperature distribution at $t = 3$ s in *unequilibrium case* for the following cases: $N_{tot} = 55$ cm^{-3} (a), $N_{tot} = 550$ cm^{-3} (b), $N_{tot} = 5500$ cm^{-3} (c). Velocity vector is shown by arrows (averaged vertical velocity is subtracted).

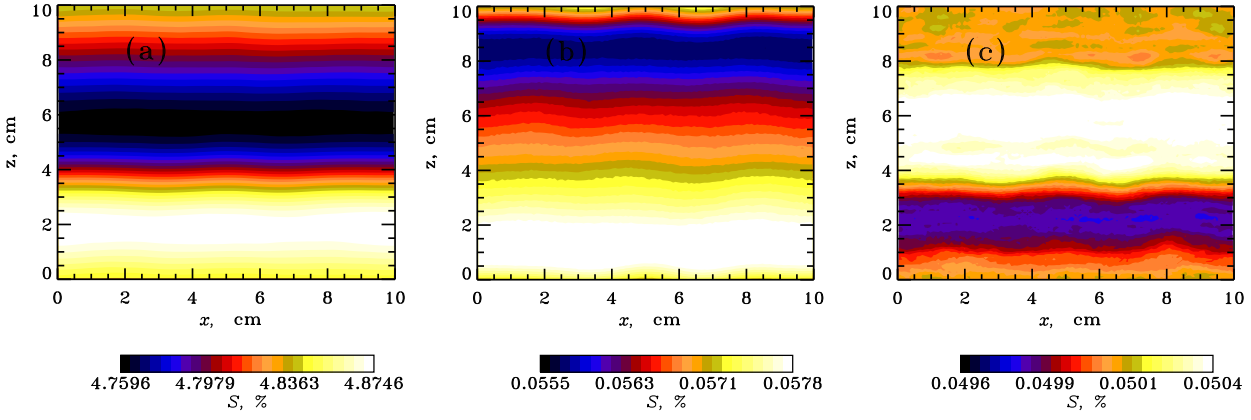

Fig. 2. Distribution of supersaturation at $t = 3$ s in the following cases: $N_{tot} = 55$ cm^{-3} (a), $N_{tot} = 550$ cm^{-3} (b), $N_{tot} = 5500$ cm^{-3} (c) in *unequilibrium* case.

provided some convincing arguments that at the cloud base high fluctuations of supersaturation on the order of up to several percent can exist. It is also well known that turbulence in high Reynolds number flows (typical in convective clouds) is highly intermittent (Siebert et al., 2010). Shaw (2000) argued that under such conditions long-living vortex tubes could produce small areas with decreased droplet number concentrations and, therefore, high supersaturation resulting in secondary activation. Summarizing, there are good arguments that supersaturation of a few percent can be generated without strong updrafts.

On the other hand, the supersaturation excess would be eliminated by condensation onto droplets and the usual equilibrium supersaturation would be restored. Therefore, the key question about the temporal time scale is under consideration now. The ratio of two time scales is important here: the phase relaxation time which describes how fast the supersaturation can react on the new thermodynamic condition and the turbulent mixing time scale which describes how fast turbulence can mix a certain volume (eddy with the length scale l). If the phase relaxation time is smaller compared to the turbulent mixing time than the quasi-steady state solution would be applicable. However, for scales where the turbulent mixing is faster we expect strong supersaturation fluctuations to "survive".

Let us now assume a small eddy of size $l = 1$ m and a local energy dissipation rate of $\epsilon = 0.1 m^2 s^{-3}$. These dissipation values are typical peak values for cumulus clouds on that small scales. The highest dissipation can be found at Kolmogorov size (see discussion in Siebert et al., 2006, 2010). The eddy turn-over time is $\tau_{eddy} = (l^2/\epsilon)^{1/3} \approx 2$ s. If we now take a phase relaxation time of the order of one second which is typical for cumulus clouds (see again Korolev and Mazin, 2003) we see that these two time scales are of the same or-

Atmos. Chem. Phys. Discuss., doi:10.5194/acp-2015-913, 2016
Manuscript under review for journal Atmos. Chem. Phys.
Published: 22 January 2016

Atmospheric Chemistry and Physics Discussions

der. Therefore, we conclude that on scales below one meter, strong supersaturation fluctuations can exist and the quasi-steady state solution is not applicable anymore. This argumentation partly follows the discussion in Section 8e by Korolev and Mazin (2003).

Kulmala et al. (1997) estimated standard deviations of supersaturation of up to 5 % based on aircraft observations at cloud level but outside the clouds. Ditas et al. (2012) observed supersaturation fluctuations in a field of stratocumulus clouds and estimated from highly collocated temperature and water vapor observations peak-to-peak values of up to 1.5 %, which is much higher compared to the quasi-steady-state solution. It is straightforward to assume that higher S values can be expected for parts of (shallow) cumulus clouds. Thus, we argue that for our small modeled volume a transient supersaturation of 10 % can be realistic for specific mixing event.

The pressure, p, is assumed to be constant everywhere in the domain and it is also based on the measurements. The air density, ρ, is calculated from the equation of state $p = \rho RT/m$, where R is gas universal constant, m is air molar mass. The initial velocity is taken to be zero.

To generate the initial turbulent field we make first 100 iterations without evaporation/activation of aerosol particles (further "aerosol dynamics"), but with included randomly directed external forces (see next section). After that the external forces are set to zero, whereas the particles start to evolve. Thus, the turbulence is decaying for the analysed time. The maximal timestep allowed by the Courant condition for convergence is $\Delta t_c = 10^{-6}$ s (Courant time step). Since Δt_c is much larger than the time step needed to move the smallest particle to the neighbour size bin ($\Delta t_a = 2 \times 10^{-7}$ s), at every Courant time step we make 5 substeps and calculate the particle evolution equation only.

Boundary conditions

In all three directions we set periodic boundary conditions for all variables, including the number density function. It means, that at every time step Δt_c the number of particles appearing on the bottom/left boundaries is equal to the number of particles disappearing through the top/right boundaries. While the periodic boundary conditions modify the initial temperature stratification, they allow us to consider this domain as an isolated volume, i.e. the total mass, energy and number of particles in the domain does not change with time. In turn, it makes possible to compare the results of simulations, varying the key parameters of the model and to carry out the detailed quantitative analysis of the interaction between aerosol and turbulence.

Basic equations

The detailed description of the main equations is presented by Babkovskaia et al. (2015). We consider the standard Navier-Stokes system including equation for conservation of mass, momentum, energy and chemical species. In the present study we modify the model, describing the evolution of aerosol number density function: water vapour pressure over a droplet of radius r is defined as (Seinfeld and Pandis, 2006; Sorjamaa and Laaksonen, 2007)

$$p_{vs} = p_0 \exp\left(\frac{A}{2r} - \frac{0.1 d_w}{2(r - r_0)}\right) \quad (1)$$

where p_0 is water vapor pressure over a flat surface at the same temperature, $A = 0.66/T$ (in μm), where $r_0 = 10$ nm is the radius of the droplet core, $d_w = 0.3$ nm is the size of water molecule.

For generation of the initial turbulence the external forces f is used in a form

$$f(\mathbf{x}, t) = Re\{N f_k(t) \exp[i\mathbf{k}(t) \cdot \mathbf{x} + i\phi(t)]\}, \quad (2)$$

where $\mathbf{x}$ is the position vector. The wave vector $k(t)$ and the random phase $-\pi < \phi(t) \leq \pi$ change at every time step; $N = f_0 c_s (|k| c_s / \Delta t_c)^{1/2}$ is the normalization factor, c_s is the sound speed, f_0 is a non-dimensional forcing amplitude; $f_k = (\mathbf{k} \times \mathbf{e}) / \sqrt{\mathbf{k}^2 - (\mathbf{k} \cdot \mathbf{e})^2}$), where $\mathbf{e}$ is an arbitrary unit vector that is real and not aligned with $\mathbf{k}$ (see detail in Pencil Code (2001)).

To study the effect of aerosol on the turbulence we consider two initial turbulent fields, taking different non-dimensional forcing amplitudes as $f_0 = 10$ (*low intensive turbulence*) and $f_0 = 100$ (*high intensive turbulence*). Also, we compare the effect of the aerosol in the case when the domain is in equilibrium with environment (*equilibrium* case) and when the temperatures inside and outside the domain are different (*unequilibrium* case), taking the environment temperature $T_0 = 285.4$ K for *equilibrium case* and $T_0 = 293$ K for *unequilibrium case* . The buoyancy force is expressed as follows

$$B = g\left[\frac{T - T_0}{T_0} + \epsilon(Y_{H_2O} - q_0) - q_c\right], \quad (3)$$

where $g = 9.81$ m s^{-2} is the acceleration of gravity, q_0 is the reference water vapor mixing ratio, $\epsilon + 1 = R_v/R_d$ is the ratio of the gas constant for water vapor and dry air, and q_c is the cloud water mixing ratio (Andrejczuk et al., 2004; Babkovskaia et al., 2015). The summary of four considered cases is in Table 2.

3 Results

Effect of total number of particles on air temperature and supersaturation distributions

In Fig. 1 we present the air temperature averaged in y-direction. In Fig. 1 (a, b, c) we present the temperature distribution in the cases where the aerosol dynamics is included. We find that without aerosol (*case 4*) after 3 s the difference

Atmos. Chem. Phys. Discuss., doi:10.5194/acp-2015-913, 2016
Manuscript under review for journal Atmos. Chem. Phys.
Published: 22 January 2016

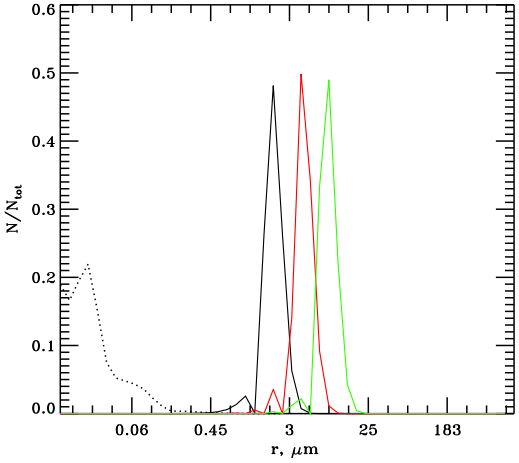

Fig. 3. Relative distribution of particles averaged over the domain at t=0 s (*black dotted curve*) and t = 3 s (*solid curve*) for the cases of $N_{\rm tot}$ = 55.5 cm^{-3} (*green solid curve*), $N_{\rm tot}$ = 555 cm^{-3} (*red solid curve*), $N_{\rm tot}$ = 5550 cm^{-3} (*black solid curve*).

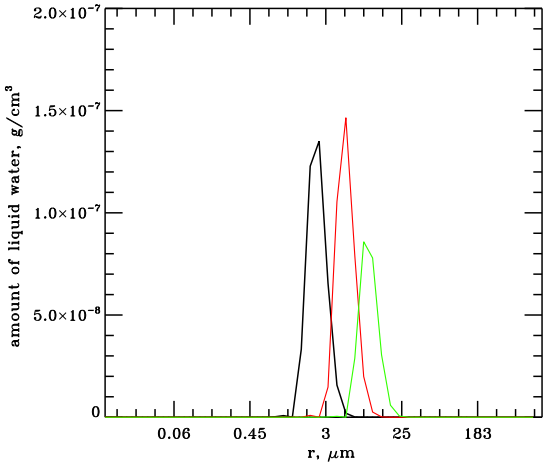

Fig. 4. Amount of liquid water accumulated in particles with corresponding radius r at t = 3 s (*solid curve*) for the cases of $N_{\rm tot}$ = 55.5 cm^{-3} (*green solid curve*), $N_{\rm tot}$ = 555 cm^{-3} (*red solid curve*), $N_{\rm tot}$ = 5550 cm^{-3} (*black solid curve*).

	case 1	*case 2*	*case 3*
N_{tot},cm^{-3}	55.5	555	5550
N_{act}, cm^{-3}	49	493	4700
LWC, g/cm^3	2.3 10^{-7}	3.69 10^{-7}	3.76 10^{-7}
Δ T, K	0.66	1.04	1.04
Δ S$_{max}$, %	-6.77	-10.5	-10.5
Δ S$_{min}$, %	-6.48	-10.13	-10.12

Table 3. Total number of particles (N_{tot}), number of activated particles (N_{act}), liquid water content (LWC), change of the temperature (Δ T), maximal values of supersaturation (Δ S$_{max}$), minimal values of supersaturation (Δ S$_{min}$) at t = 3 s for three considered cases. *Unequilibrium* case is considered.

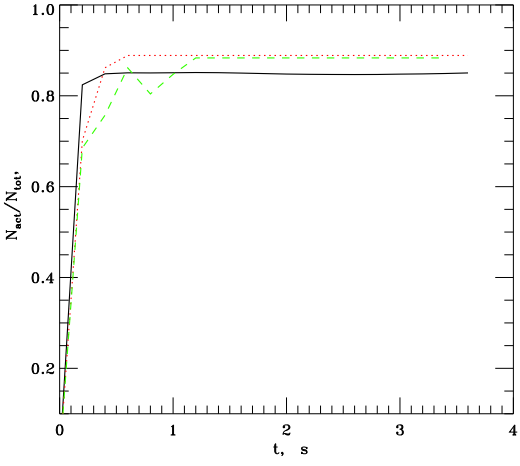

Fig. 5. Relative number of activated particles as a function of time $N_{\rm tot}$ = 55.5 cm^{-3} (*green curve*), $N_{\rm tot}$ = 555 cm^{-3} (*red curve*), $N_{\rm tot}$ = 5550 cm^{-3} (*black curve*).

between the absolute value of maximal (285.381 K) and minimal (285.380 K) temperatures in the domain is still about 0.001 K, while in *case 3* this difference achieves 0.02 K (see Fig. 1, d). Moreover, the temperature increases by about 1 K everywhere in the domain because of condensation of water vapor on aerosol particles.

Changing of temperature distribution with time is mostly attributable to the periodic boundary conditions: the coldest layers are moving from the bottom to the middle of the domain. However, comparing (a), (b) and (c) panels in Figs. 1 and Fig. 2 we note that the positions of the coldest layers in different panels are different. The coldest layers in case of $N_{\rm tot}$ = 55 cm^{-3} coincide with the layers where supersaturation is minimal (see panel a), whereas for other two cases, $N_{\rm tot}$ = 555 cm^{-3} (b) and 5550 cm^{-3} (c), the coldest layers correspond to the positions where supersaturation

Atmos. Chem. Phys. Discuss., doi:10.5194/acp-2015-913, 2016
Manuscript under review for journal Atmos. Chem. Phys.
Published: 22 January 2016

Atmospheric Chemistry and Physics Discussions

achieves maximum. It happens because of the different effect of aerosol dynamics in dependence of $N_{\rm tot}$. The small amount of aerosol particles (*case 1*) does not make any substantial effect on the temperature distribution, i.e. both temperature and supersaturation are identically shifting with time in vertical direction. In turn, in *cases 2* and *3* aerosol dynamics crucially changes the temperature distribution. One can see in Figs. 1, 2 that layers with larger temperature correspond to layers with smaller supersaturation. It can be interpreted as follows. More intensive condensation occurs in initially warmer layers because supersaturation is larger there and respectively the temperature grows faster in these layers. In turn, since supersaturation exponentially depends on temperature, $S \propto \exp(-T)$, at some moment S appears to be smaller in warmer than cooler layers. Thus, equilibrium supersaturation is higher in the layers with temperature minimum (and vice versa). Also, we find that in *case 1* at $t = 3$ s the supersaturation is about 5 % and the aerosol is still activating, whereas in *case 3* for the first 3 s the supersaturation almost drops to zero and the system is coming to an equilibrium.

Additionally, we investigate how fast the system with initially high value of supersaturation ($S = 10$ %) comes to an equilibrium ($S = 0$ %) in dependence on different total numbers of droplets to answer the question how $N_{\rm tot}$ affects the phase relaxation time. Analysing Fig. 2 we find that in a case of $N_{tot} = 55$ cm^{-3} it takes more than 3 s for the system to come to equilibrium, i.e. phase relaxation time appears to be larger than theoretically estimated turbulent mixing time ($\tau_{eddy} = 2$ s) (see discussion in section 2). Thus, strong supersaturation fluctuations can "survive" longer if the total number of droplets is smaller.

Effect of total number of particles on activation

In this study we consider that all particles with radius larger than $r_{cr} = 1.75$ μm are activated. This value is somewhat arbitrary but the results of our study were not sensitive on the choice of r_{cr} provided that $r_{cr} \leq 1.75$ μm. In Fig. 3 we present the normalized particle distribution at $t = 0$ s and $t = 3$ s. We find that the smaller is the total number, the larger particles are produced for the similar time period. Comparing the supersaturation at $t = 3$ s in these three cases (Fig. 2) one can see that in the case of the largest N_{tot} the supersaturation appears to be close to zero and particles stop to grow, while for the smaller N_{tot} the supersaturation is about 3 % and particles continue growing. Therefore, the system is coming to an equilibrium (i.e. $S = 0$) faster and aerosol particles cease to grow earlier for the larger N_{tot}. Thus, our DNS results for a case without vertical displacement and resulting convective cooling confirm the Twomey effect and show that aerosol particles can grow and possibly achieve the size of the rain drop only in the case of small total number of particles. This is consistent with the fact that in natural clouds, deep ascent is needed to drive the prolonged condensational growth of drops, in order for rain to form (e.g. Rogers and Yau 1989,

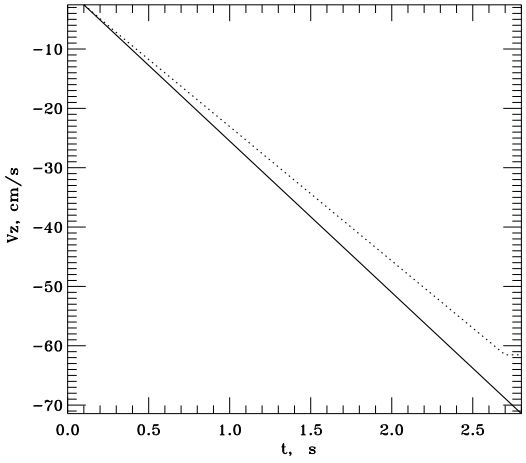

Fig. 6. Averaged vertical velocity as a function of time with aerosol for $N_{\rm tot} = 5500$ cm^{-3} (*dotted curve*); and without aerosol (*solid curve*). *Unequilibrium* and *low intensive turbulence* case is considered (see Table 3).

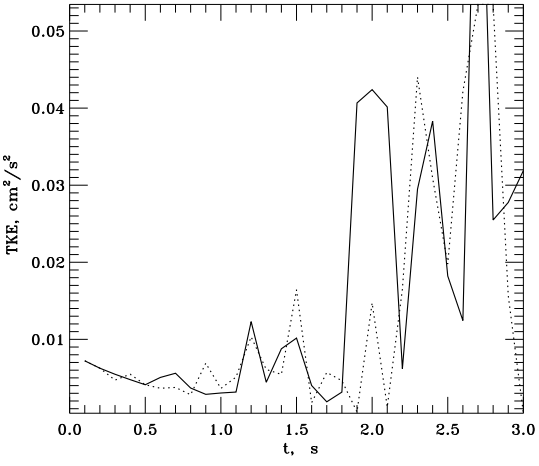

Fig. 7. The dependence of the average kinetic energy on time with aerosol for $N_{\rm tot} = 5500$ cm^{-3} (*dotted curve*); and without aerosol (*solid curve*). The other parameters correspond to *unequilibrium* case with *low intensive turbulence* (see Table 2).

Atmos. Chem. Phys. Discuss., doi:10.5194/acp-2015-913, 2016
Manuscript under review for journal Atmos. Chem. Phys.
Published: 22 January 2016

Atmospheric Chemistry and Physics Discussions

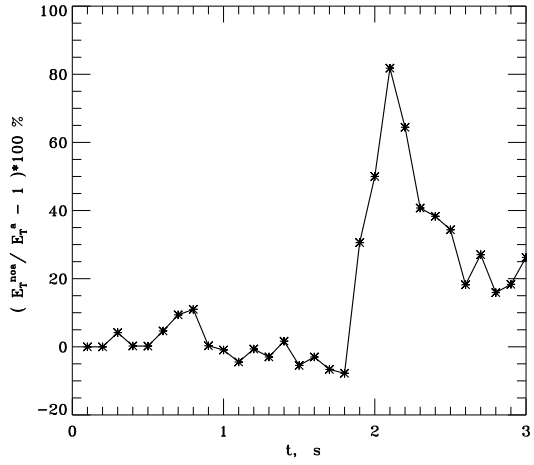

Fig. 8. The difference between turbulent kinetic energy averaged over time period t in a case without aerosol (E_T^{noa}) and with aerosols (E_T^a), where $E_T(t) = 1/t \int_0^t TKE(t')dt'$. All other parameters are the same as in Fig.7.

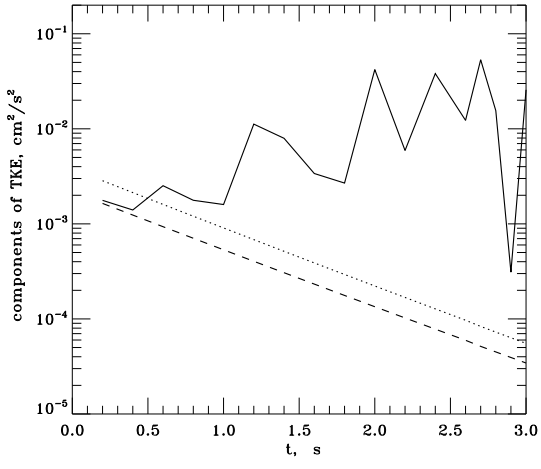

Fig. 9. The dependence of the x-component (*dotted curve*), y-component (*dashed curve*) and z-component (*solid curve*) of the averaged kinetic energy on time with aerosol for $N_{\text{tot}} = 5500$ cm^{-3}.

a short course in cloud physics). In real clouds, the ascent is the source of larger-scale supersaturation. One should also mention, that in the scope of this model we neglect collision and coalescence of aerosol particles, which can be crutial in creation of rain drops.

In addition, in Fig. 4 we analyse the amount of liquid water, $LW(r) = 4/3\pi r^3 \rho_w N(r)$, on particles with radius r (where $N(r)$ is the number of particles with radius r, ρ_w is liquid water density) and in Fig. 5 we show the number of activated particles averaged over the domain as a function of time in *cases 1, 2, 3*. In Table 3 we collect the most important quantities, such as number of activated particles, liquid water content $LWC = \int LW(r)/\Delta r\, dr$ (where Δr is a size of corresponding bin), and the changes of temperature and supersaturation averaged over domain at $t = 3$ s for *cases 1, 2, 3*.

We find that while the total number in *case 2* is ten times smaller than in *case 3*, liquid water content is similar in these two cases. On the other hand, *LWC* appears to be smaller in *case 1* than in *cases 2, 3* (see Table 3 and Fig. 4). It happens because the probability of water molecules to catch a particle is much smaller in a case of the smallest particle concentration (*case 1*) than in *cases 2, 3*. In Fig. 5 one can see that in *case 1* and *case 2* the number of activated particles does not grow after 1.2 s and 0.6 s, correspondingly, and in *case 3* it happens after 0.4 s. Since in *case 3* the equilibrium is achieved earlier than in *cases 1* and *2*, the maximum of final particle distribution in *case 3* is shifted (see Fig. 3) and the final relative number of activated particles appears to be smaller than in *cases 1* and *2*. We find that the number of activated particles approximately linearly depends on the total number, whereas the change of N_{tot} in 100 times leads to increase of *LWC* just by 40 % (Table 3).

Effect of aerosol on the turbulent motion

We analyse the effect of aerosol on the turbulent motion. First, we consider the *equilibrium case*, taking $T_0 = 285.4$ K and $q_0 = 0.0124$ in Eq. 3. In that case the turbulent field appears to be isotropic. Next, we increase $T_0 = 293$ K and study the developing of turbulence in *unequilibrium case*. Then the intensive vertical motion is generated because of buoyancy force. Note, that the model domain is not vertically displaced during the simulation time but the vertical motion is generated within domain. Also, we vary parameter f_0 in Eq. 2 to compare the developing of *low intensive* ($f_0 = 10$) and *high intensive* ($f_0 = 100$) turbulence in both *equilibrium* and *unequilibrium* cases. The summary of parameters is presented in Table 2. Finally, we compare the results of simulations with particles (taking $N_{tot} = 5500$ cm^{-3}) and without them in all four cases described above.

We find that the vertical motion of air is decelerated because of aerosol dynamics. Also, in Fig. 8 we show the time averaged turbulent kinetic energy, $E_T(t) = 1/t \int_0^t TKE(t')dt'$, as a function of time in the case with aerosol particles and

Atmos. Chem. Phys. Discuss., doi:10.5194/acp-2015-913, 2016
Manuscript under review for journal Atmos. Chem. Phys.
Published: 22 January 2016

Atmospheric Chemistry and Physics Discussions

without them. We conclude that turbulence is damped because of presence of aerosols. We interpret these results as follows. The air temperature increases because of latent heating caused by condensation onto drops, and the temperatures inside and outside the domain is reduced. It results in decreased buoyancy force and deceleration in vertical direction. Thus, we conclude that aerosol affects the turbulence via buoyancy.

Also, we find that deceleration does not depend on intensity of turbulent fluctuations, i.e. deceleration in vertical direction is the same in *low intensive turbulence* and *high intensive turbulence* cases. Moreover, turbulent fluctuations are damped because of presence of aerosol particles in all four considered cases. However, the damping effect is stronger in *unequilibrium* with *low intensive turbulence* than in other three cases. The dependences of vertical velocity and turbulent kinetic energy (TKE) averaged over the domain as a function of time for *unequilibrium* case with *low intensive turbulence* are presented in Figs. 6 and 7, correspondingly.

Finally, we find that there is a strong variation of TKE with time (see Fig. 7). To interpret this fact we plot x- ,y- and z- components of TKE in Fig. 9 and find strong time variations only in z-component of TKE (x- and y- components are smoothly decreasing with time). We conclude that it results from fluctuations of temperature caused by aerosol dynamics, and therefore, changes of buoyancy force with time, which results in perturbation of vertical motion.

4 Summary

Turbulence, aerosol growth and microphysics of hydrometeors in clouds are intimately coupled. In the present study a new modelling approach was applied so as to quantify this linkage. This model represents the 3D fluid flow on the microscale inside a volume of 10 cm x 10 cm x 10 cm, just inside the cloud in the mid-troposphere. We study the interaction in the cloud area under transient, high supesaturation conditions, using direct numerical simulations. As the initial conditions we take the observational data obtained by the ACTOS platform. To analyse the effect of aerosol on the turbulence we choose the part of the cloud where the supersaturation is about 10 % and condensation is the dominant process. As an initial distribution of particles we take the data of measurements at the sea level and analyse the drops activated by the aerosols in simulations.

We compare the results of simulations with particles and without them. We find that the total number of particles in the domain is crucial for distribution of temperature and for developing of turbulence. Even small amount of aerosol particles (55.5 cm^{-3}) increases the air temperature by 1 K because of latent heating caused by condensation onto drops. The system comes to an equilibrium faster for the larger total number of particles. Also, we find that the larger is N_{tot} the smaller is the relative number of activated particles (averaged over the domain). Analysing the effect of aerosol dynamics on the turbulent kinetic energy and on vertical velocity we conclude that the presence of aerosol has an effect on vertical motion and in our case tends to reduce downward velocity. We conclude that aerosols quite strongly influences the dynamics in the cloud area. Such effect of aerosols can be crucial also for large scales usually studied with Large Eddy Simulation (LES) and the LES parametrization can be improved with direct numerical simulations.

Acknowledgments

We thank the Helsinki University Centre for Environment (HENVI) and computational resources from CSC – IT Center for Science Ltd are all gratefully acknowledged. This research is supported by the Academy of Finland Center of Excellence program (project number 272041). Anthropogenic emissions on Clouds and Climate: towards a Holistic UnderStanding" (BACCHUS), project no. 603445.

REFERENCES

Andrejczuk, M., Grabowski, W., Malinowski, S., Smolarkiewicz, P.,2004. Numerical simulations of Cloud-clear air interfacial mixing. J. Atmos. Sci., 61, 1726-1739.

Babkovskaia, N., Boy, M., Smolander, S., Romakkaniemi, S., Rannik, U., Kulmala, M., 2015. A study of aerosol activation at the cloud edge with high resolution numerical simulations, Atmospheric Research, 153, 49–58.

Babkovskaia, N., Haugen, N., Brandenburg, A., 2011. A high-order public domain code for direct numerical simulations of turbulent combustion. J. of Computational Physics, 230, 1-12.

Benmoshe, N., Khain, A. P., 2014. The effects of turbulence on the microphysics of mixed-phase deep convective clouds investigated with a 2-D cloud model with spectral bin microphysics. J. Geophys. Res. Atmos., 119, 207-221.

Ditas, F., Shaw, R.A., Siebert, H., Simmel, M., Wehner, B., and Wiedensohler, A. Aerosols-cloud microphysics-thermodynamics-turbulence: evaluating supersaturation in a marine stratocumulus cloud. Atmos. Chem. Phys., 12(doi:10.5194/acp-12-2459-2012), 2459–2468.

Dobler W., Stix M., Brandenburg, A., 2006. Magnetic field generation in fully convective rotating spheres Astrophys. J., 638, 336-343.

Easter, R.C. and L.K. Peters, 1994. Binary homogeneous nucleation: Temperature and relative humidity fluctuations, nonlinearity and aspects of new particle production in the atmosphere J. Appl. Meteorol. 33, 775-784.

Forster, P., 2007. Changes in atmospheric constituents and in radiative forcing Climate Change 2007: The Physical Science Basis, S. Solomon et al., Eds., Cambridge University Press, 129–234.

Haugen N. E., Brandenburg, A., 2006. Hydrodynamic and hydromagnetic energy spectra from large eddy simulations Phys. Fluids, 18, 1-7.

Katzwinkel, J., Siebert, H., Heus, T., Shaw, R. A., 2014 Measurements of turbulent mixing and subsiding shells in trade wind cumuli J. Aerosol Sci., 71, 2810-2822.

Atmos. Chem. Phys. Discuss., doi:10.5194/acp-2015-913, 2016
Manuscript under review for journal Atmos. Chem. Phys.
Published: 22 January 2016

Atmospheric Chemistry and Physics Discussions

korolev, A. V. and M. Mazin, I.P., 2003. Supersaturation of Water Vapor in Clouds J. Atmos Sci., 60, 2957-2974, 2003.

Kulmala, M., Rannik, U., Zapadinski, E., Clement., C.F., 1997. The effect of saturation fluctuations on droplet growth J. Aerosol Sci., 28, 1395-1409.

Mellado, J. P., 2010. The evaporatively driven cloup-top mixing layer. J. Fluid Mech., 660, 5-36.

Nilsson, E. D. and Kulmala, M., 1998. The potential for atmospheric mixing processes to enhance the binary nucleation rate J. Geophys. Res. 103, 1381-1389.

Nilsson, E. D., Pirjola, L., and M. Kulmala, 2000. The effect of atmospheric waves on aerosol nucleation and size distribution J. Geophys. Res. 105, 19917-19926.

The PENCIL Code, http://pencil-code.googlecode.com, 2001.

Poinsot, T., J., and Lele S., K., 1992. Boundary conditions for direct simulations of compressible viscous flow. J. Comp. Phys., 101, 104-139.

Romakkaniemi, S., G. McFiggans, K. N. Bower, P. Brown, H. Coe, and T. W. Choularton, 2009. A comparison between trajectory ensemble and adiabatic parcel modeled cloud properties and evaluation against airborne measurements. J. Geophys. Res., 114, D06214.

Rogers, R.R. and Yau, M.K., 1989. A short course in cloud physics 3rd edition, 1989. Pergamon Press

Seinfeld, J. H. and Pandis S. N., 2006. Atmospheric chemistry and physics: From Air pollution to Climate Change. (John Wiley & Sons, Inc).

Siebert, H., Beals, M., Bethke, J., Bierwirth, E., Conrath, T., Dieckmann, K., Ditas, F., Ehrlich, A., Farrell, D., Hartmann, S., Izaguirre, M. A., Katzwinkel, J., Nuijens, L., Roberts, G., Schäfer, M., Shaw, R. A., Schmeissner, T., Serikov, I., Stevens, B., Stratmann, F., Wehner, B., Wendisch, M., Werner, F., and Wex, H., 2013. The fine-scale structure of the trade wind cumuli over Barbados – an introduction to the CARRIBA project (11 Oct 2013). Atmos. Chem. Phys., 13, 10061-10077.

Siebert, H., Lehmann, K., Wendisch, M., 2006. Observations of small scale turbulence and energy dissipation rates in the cloudy boundary layer. J. Atmos. Sci., 63, 1451-1466.

Siebert, H., Shaw, R. A., Warhaft, Z., 2010 Statistics of Small-Scale Velocity Fluctuations and Internal Intermittency in Marine Stratocumulus Clouds. J. Atmos. Sci., 67, 262–273.

Sorjamaa, R., Laaksonen, A., 2007. The effect of H_2O absorption on cloud drop activation of insoluble particles: a theoretical framework. Atmos. Chem. Phys., 7, 6175-6180.

Shaw, R. A., 2000. Supersaturation intermittency in turbulent clouds. J. Atmos. Sci., 57, 3452–3456.